Supplement to “Extreme warming restructures habitat distribution and productivity along local gradients in stress and biodiversity” v1

Matthew Whalen[1]

[1]Affiliation not available

June 4, 2021

Supplemental Material

Table S1. Range of sampling dates for intertidal biodiversity surveys in each year

Year	Date range		
2012	03 July	-	05 July
2013	23 May	-	26 May
2014	12 June	-	14 June
2015	14 June	-	16 June
2016	05 June	-	07 June
2017	24 May	-	26 May
2018	12 June	-	14 June
2019	01 June	-	04 June

Regional measures of sea surface temperature, atmospheric temperatures, and waves

The 2014-2016 marine heatwave began with the formation of a warm ‘blob’ off of the west coast of North America, which was followed by an intense El Niño (Di Lorenzo & Mantua 2016). This led to a multiyear MHW that was strongly felt along Central Coast BC. Air and water temperature measurements from three BC lightstations illustrate the scale and severity of the heatwave in this region (Fig. 1). The heatwave was sustained from May 2014 to November 2017, longer than sites further south (e.g., California and Mexico: (Arafeh-Dalmau *et al.* 2019; Sanford *et al.* 2019) but consistent with patterns elsewhere on the BC coast (Starko *et al.* 2019). In a similar fashion, air temperatures were anomalously high from early 2014 through the end of 2016, demonstrating that this heatwave was extreme both oceanographically and atmospherically (Swain *et al.* 2017). This MHW rivaled the severity of the 1997/1998 El Niño for both air and water temperature in this region and represents the longest set of heatwaves in a time series of SST dating to the 1930s (Fig. S1). During the heatwave, daily SST and air temperature anomalies regularly exceeded 2.5°C.

Atmospheric temperatures on Calvert Island during the study period also reflect the anomalous conditions of the 2014-2016 NE Pacific MHW (Fig. S4). Temperatures tended toward positive temperature anomalies relative to mean conditions from Fall 2014 through Spring 2016.

Local intertidal temperatures

Temperature loggers were wrapped in parafilm and placed inside a PVC cap that was spray painted black and fastened to the substratum using a bolt, wall-anchor and marine epoxy. Temperature was then logged every 4 hours. From July 2012 to May 2013, we also measured intertidal temperatures in the high zone at Foggy Cove, but the cap was the blue top from a Falcon tube (Fisher Scientific). We anticipate differences due to the material of the cap, how it was affixed to the rock, and the precise location of the logger, therefore we do not formally compare 2012-2013 data with those from 2014-2016.

Temperature data collected *in situ* during the study were not sampled over a sufficiently long time period to allow similar retrospective analysis as we performed with data from BC lightstations, but they offer a glimpse into local temperatures during the heatwave that are relevant to intertidal organisms, as well as important differences in thermal environments among sites. Local intertidal temperatures measured in one transect from Foggy Cove before (2012-2013) and during the heatwave (2014- 2016) spanned a range of over 30degC (Fig. S3). Winter temperatures from 2015 were 1degC warmer than the winter of 2016. Additionally, *in situ* temperatures in the late summer of 2015 more often exceeded the 75th quartile than in 2014, suggesting that high intertidal conditions in 2015 was more stressful than in 2014. Although we cannot directly compare the temperature data from before and during the heatwave, our data suggest that variance in intertidal temperatures may have increased during the heatwave. Rock temperatures were also highly variable across the three sites in our study area based on data from 2015-2016 (Fig. S4). North Beach experienced much longer durations of temperatures exceeding 20deg and 30degC than either other site, while Fifth Beach was the only site to never experience in situ temperatures exceeding 30degC during the 2015 deployment. These differences are likely attributable to the physical setting of each site. North Beach faces west and has no barriers to sunlight on clear days, while Fifth Beach faces north and is backed by a vegetated bluff that blocks direct sunlight for much of the day. Foggy Cove differs from the two other sites in that its slope is shallower than the other sites and is characterized by boulders rather than a contiguous rocky outcrop, suggesting a different abiotic stress gradient over similar spatial extents (Fig. S1).

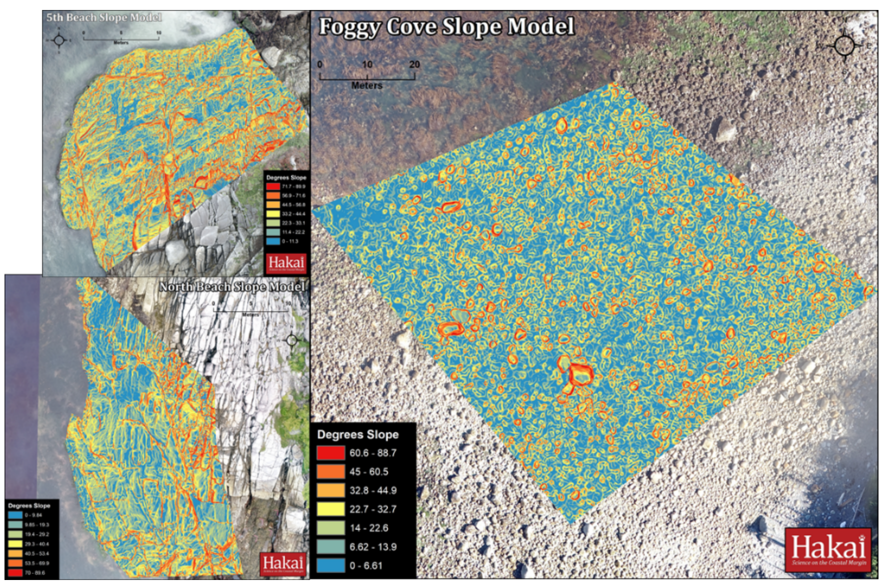

Fig. S1. Digital elevation models for the three sites in this study. Colors in all panels represent local slope estimates ranging from 0 to 90 degrees, where 0 degrees is parallel with a level horizontal plane. Note that the spatial scale of the image is different for Foggy Cove.

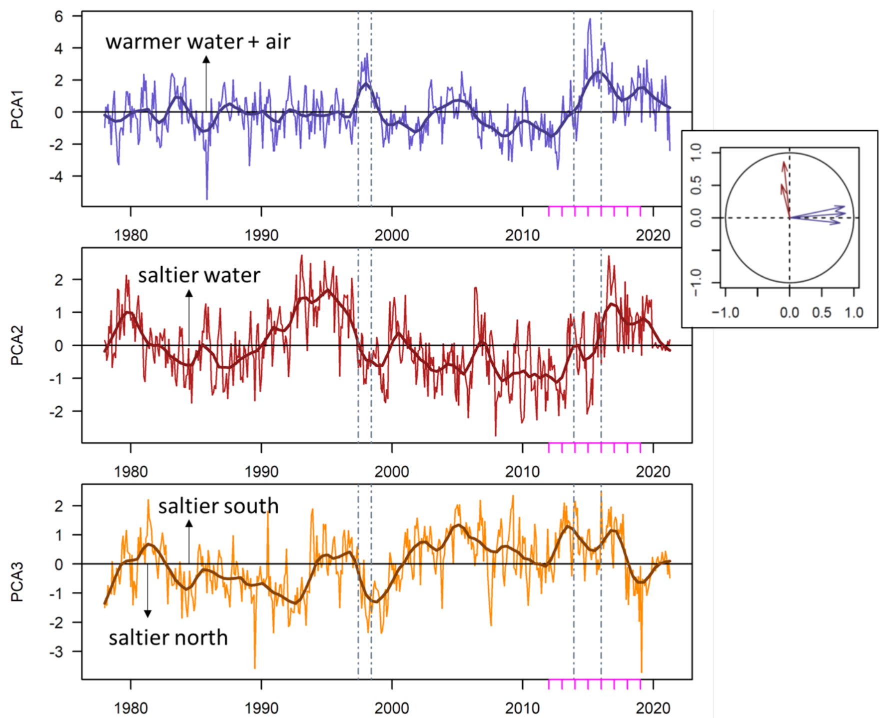

Fig. S2. Temporal change in the first three axes of a principal components analysis (PCA) on five environmental variables: monthly temperature anomalies at three lightstations (sea surface temperature at Pine and McInnes Islands, air temperature at Addenbroke Island) and moshtly surface salinity anomalies at Pine and McInnes Islands. The PCA used only times shared by all datasets (1978-2020), but anomalies are calculated from all available data. Lighter lines show monthly PCA values, while the darker lines are LOESS smoothers. Survey years are noted with magenta tick marks. Note how anomalous conditions continued in the region, even after the 2014-2016 marine heatwave ended elsewhere.

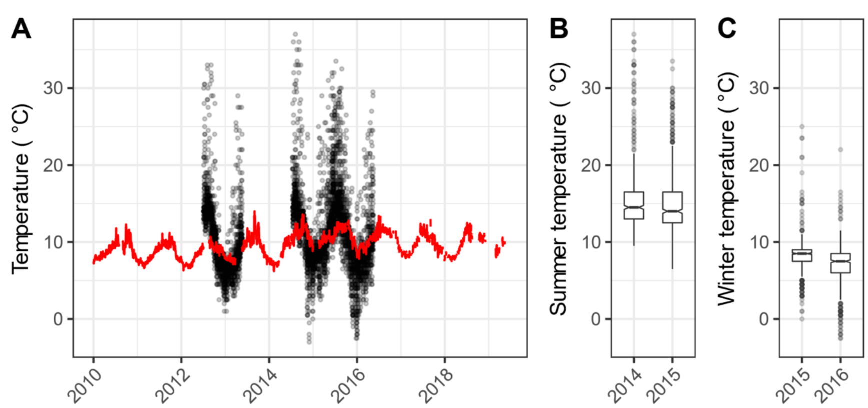

Fig. S3. (A) comparison of *in situ* temperature data from Foggy Cove (black points) and SST data from the Pine Island lightstation (red line; see Fig. 1, Fig. S2). Individual temperature records are shown for both datasets: *in situ* data were collected every 4 hours, while lightstation SST is recorded once daily when a keeper is present. Boxplots show the distributions of summer (B, July through September) and winter (C, December through February) *in situ* temperatures at Foggy Cove from 2014 to 2016.

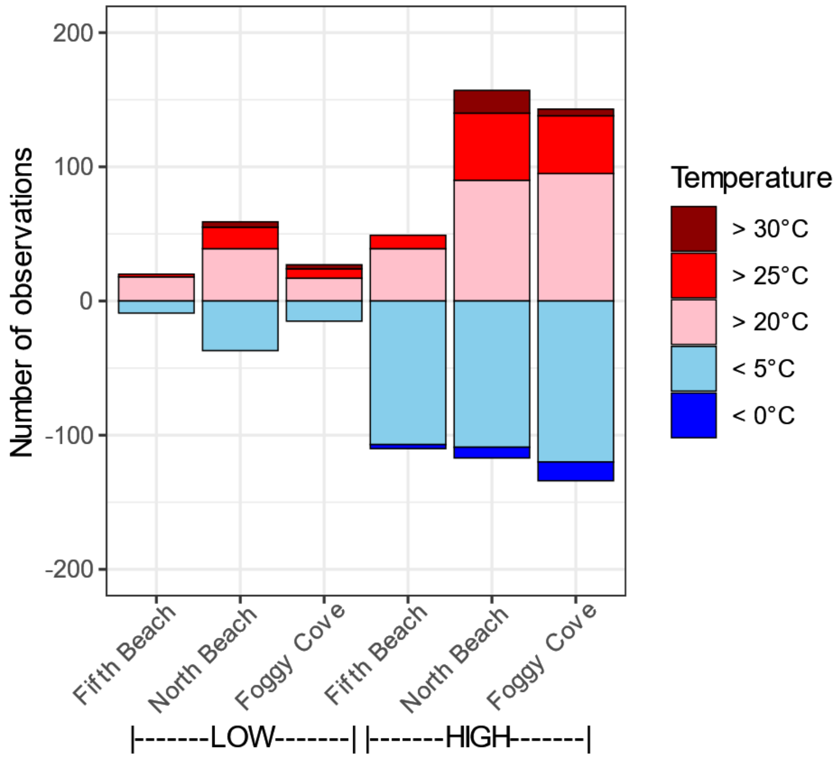

Fig. S4. Temperature logger measurements collected between June 2015 and May 2016 in LOW and HIGH zones at each study site. Bars show the number of observations (taken every four hours) above and below several thresholds for each logger.

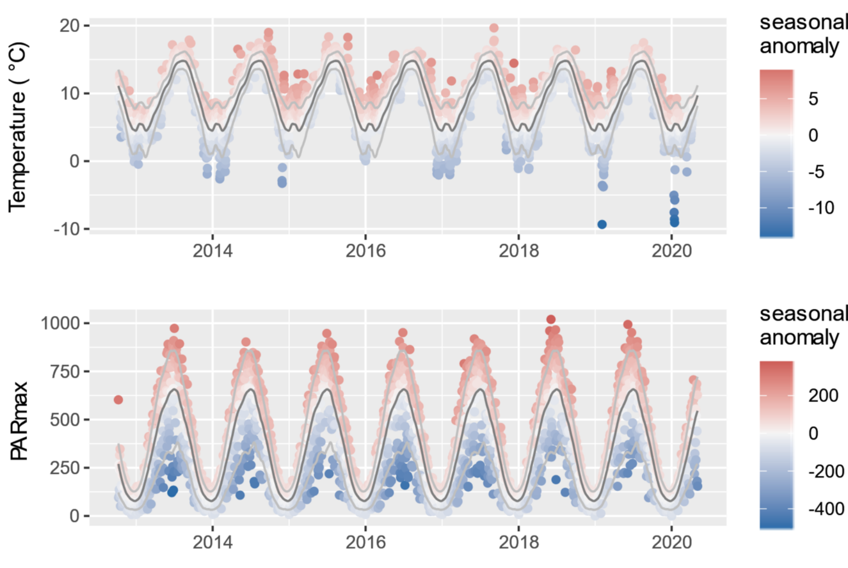

Fig. S5. Hourly atmospheric temperature and hourly maximum photosynthetically active radiation (PARmax) records collected since October 2012 at a weather station on Calvert Island. Black line shows the seasonal trends, and color of data points represent anomalies from the seasonal trend. The weather station is located above Foggy Cove at 63m above sea-level at the top of a nearby hill that is often above the fog layer

Selection of taxa: Because we were interested in modelling species abundance as a function of year, we could only include species that occurred fairly regularly. The rarest taxa were not included in the joint species distribution modeling with HMSC. We could have included those species, but we would have had far less certainty about distributional patterns in any one year, as well as patterns across years. Therefore, we set an arbitrary threshold that species must have occurred in at least 48 plots throughout the entire time series, which equates to an average of 6 quadrats per year. This threshold left a minimum of XX observations in any year and a minimum of XX percent cover in any year.

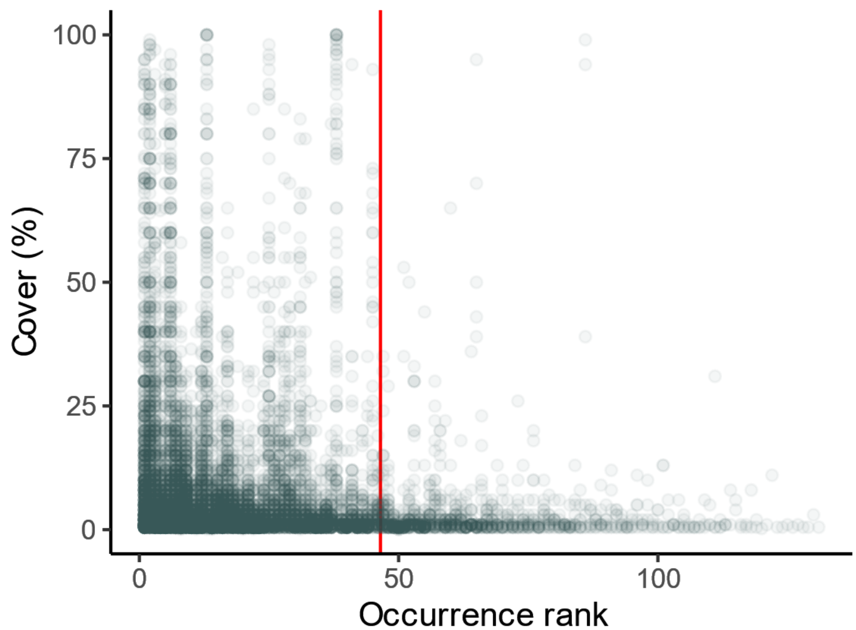

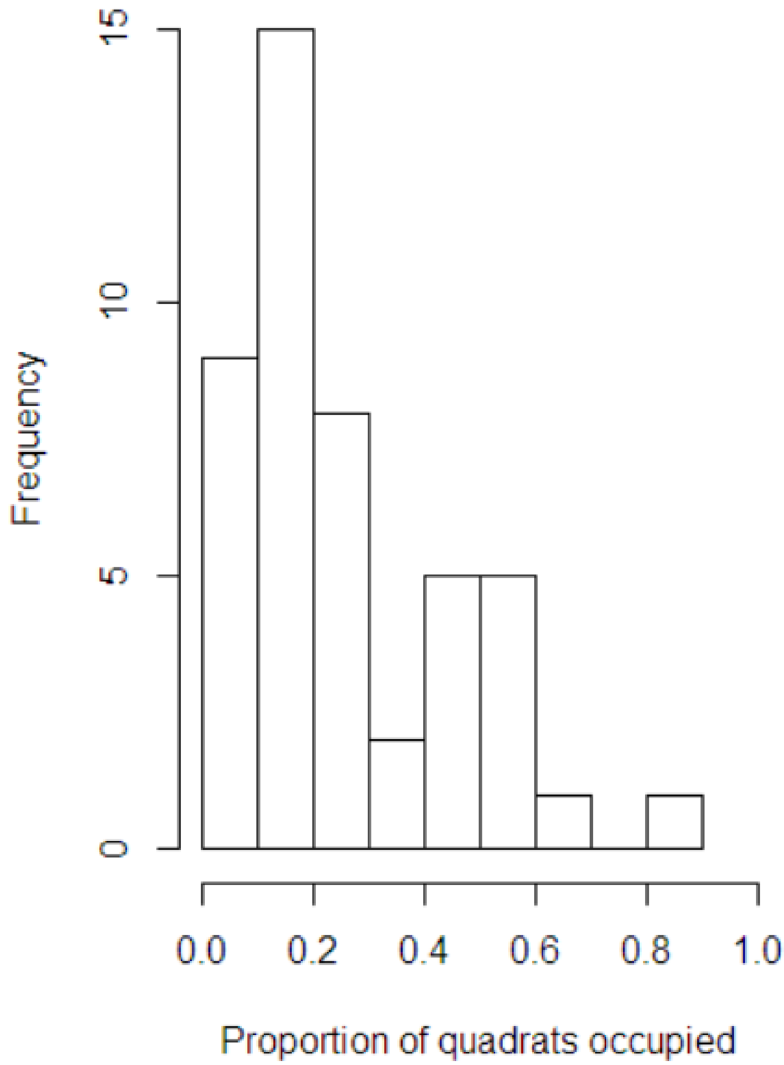

Fig. S6. Summary of cover for all taxa ordered by average occurrence in the dataset. The red line shows the threshold for inclusion in HMSC analysis. The inset figure shows the frequency of occurrence across taxa.

Supplemental Table 2. List of all taxonomic names used in the analyses. Taxa used in HMSC modeling are the first 47 taxa, while other taxa were used in analyses of total cover, species richness, and community composition. The trophic position and functional group designation of each taxon is also provided.

	rank	**taxon**	**HMSC**	**trophic position**	**functional group**
1	1	*Hildenbrandia* spp.	yes	producer	crust
2	2	*Fucus distichus*	yes	producer	canopy

3	3	*Pyropia* spp.*	yes	producer	blade
4	4	*Mastocarpus* spp.	yes	producer	turf
5	5	*Mastocarpus* spp. (crustose “Petrocelis” phase)	yes	producer	crust
6	6	Barnacles**	yes	consumer	animal
7	7	*Corallina* spp.	yes	producer	turf
8	8	*Endocladia muricata*	yes	producer	thin turf
9	9	*Chamberlainium tumidum*	yes	producer	crust
10	10	*Ulva* spp.	yes	producer	blade
11	11	*Halosaccion glandiforme*	yes	producer	turf
12	12	articulate *Bossiella* spp.	yes	producer	animal
13	13	*Alaria marginata*	yes	producer	canopy
14	14	*Acrosiphonia* spp.	yes	producer	thin turf
15	15	Anemone	yes	consumer	animal
16	16	coralline crust	yes	producer	animal
17	17	*Plocamium violaceum*	yes	producer	thin turf
18	18	*Mazzaella oregona*	yes	producer	blade
19	19	*Microcladia borealis*	yes	producer	thin turf
20	20	*Callithamnion pikeanum*	yes	producer	thin turf
21	21	*Cryptosiphonia woodii*	yes	producer	turf
22	22	*Gloiopeltis furcata*	yes	producer	thin turf
23	23	*Leathesia marina*	yes	producer	turf
24	24	*Hymenena* spp.	yes	producer	turf
25	25	*Phyllospadix* spp.	yes	producer	canopy
26	26	*Polyneura latissima*	yes	producer	turf
27	27	*Mazzaella splendens*	yes	producer	blade
28	28	*Neorhodomela larix*	yes	producer	turf
29	29	*Ptilota filicina*	yes	producer	thin turf
30	29	*Savoiea robusta*	yes	producer	thin turf
31	31	*Mytilus* spp.	yes	consumer	animal
32	32	*Odonthalia floccosa*	yes	producer	turf
33	33	*Elachista fucicola*	yes	producer	thin turf
34	34	*Cladophora columbiana*	yes	producer	thin turf
35	34	*Lithothamnion phymatodeum*	yes	producer	crust
36	34	*Ralfsioid*	yes	producer	crust
37	37	*Polysiphonia* spp.	yes	producer	thin turf
38	38	*Hedophyllum sessile*	yes	producer	canopy
39	39	*Ceramium pacificum*	yes	producer	thin turf
40	40	*Neopolyporolithon reclinatum*	yes	producer	crust
41	41	*Neogastroclonium subarticulatum*	yes	producer	turf
42	42	*Mazzaella parvula*	yes	producer	turf
43	43	*Prionitis* spp.	yes	producer	turf
44	44	*Farlowia mollis*	yes	producer	turf
45	45	*Egregia menziesii*	yes	producer	canopy
46	46	*Dilsea californica*	yes	producer	blade
47	47	*Palmaria hecatensis*	yes	producer	blade
48	48	*Codium fragile*	no	producer	turf
49	49	*Nemalion helminthoides*	no	producer	turf
50	49	Tube worms	no	consumer	animal
51	51	*Analipus japonicus*	no	producer	turf
52	52	Bryozoan	no	consumer	animal
53	52	*Schizymenia pacifica*	no	producer	blade

54	52	Tunicata/Porifera	no	consumer	animal
55	55	*Scytosiphon lomentaria*	no	producer	turf
56	56	*Codium setchellii*	no	producer	crust
57	56	*Hedophyllum nigripes*	no	producer	canopy
58	58	*Costaria costata*	no	producer	canopy
59	58	*Ectocarpus commensalis*	no	producer	thin turf
60	58	*Osmundea spectabilis*	no	producer	turf
61	61	*Peyssonnelia* sp.	no	producer	crust
62	62	*Blidingia* sp.	no	producer	turf
63	62	*Palmaria mollis*	no	producer	blade
64	64	*Dactylosiphon bullosus*	no	producer	turf
65	64	*Scytosiphon dotyi*	no	producer	turf
66	66	*Calliarthron tuberculosum*	no	producer	turf
67	67	*Tokidadendron bullatum*	no	producer	turf
68	68	Unknown crust	no	producer	crust
69	69	*Salishia firma*	no	producer	blade
70	70	*Ahnfeltia fastigiata*	no	producer	turf
71	70	*Chiharaea silvae*	no	producer	turf
72	70	*Cumathamnion decipiens*	no	producer	turf
73	70	*Lomentaria hakodatensis*	no	producer	turf
74	70	*Mazzaella parksii*	no	producer	turf
75	70	*Melanosiphon intestinalis*	no	producer	turf
76	70	*Pollicipes polymerus*	no	consumer	animal
77	77	*Colpomenia peregrina*	no	producer	turf
78	77	*Desmarestia ligulata*	no	producer	canopy
79	77	*Laminaria setchellii*	no	producer	canopy
80	80	*Chiharaea rhododactyla*	no	producer	turf
81	81	*Antithamnionella* spp.	no	producer	thin turf
82	81	*Melobesia* sp.	no	producer	crust
83	81	*Smithora naiadum*	no	producer	blade
84	84	*Antithamnion defectum*	no	producer	thin turf
85	84	*Johansenia macmillanii*	no	producer	turf
86	86	*Erythrotrichia carnea*	no	producer	thin turf
87	86	*Nereocystis luetkeana*	no	producer	canopy
88	86	*Pylaiella littoralis*	no	producer	thin turf
89	89	*Collinsiella tuberculata*	no	producer	turf
90	89	Hydroid	no	consumer	animal
91	89	*Neorhodomela oregona*	no	producer	turf
92	89	*Rhodochorton purpureum*	no	producer	thin turf
93	93	*"Bangia"* sp.	no	producer	thin turf
94	93	*Cladophora sericea*	no	producer	thin turf
95	93	*Laminaria yezoensis*	no	producer	canopy
96	93	*Rhizoclonium tortuosum*	no	producer	thin turf
97	97	*Desmarestia aculeata*	no	producer	turf
98	97	*Herposiphonia plumula*	no	producer	turf
99	97	*Lithothamnion glaciale*	no	producer	crust
100	97	*Opuntiella californica*	no	producer	blade
101	97	*Pododesmus* sp.	no	consumer	animal
102	97	*Soranthera ulvoidea*	no	producer	turf
103	97	*Sphacelaria rigidula*	no	producer	thin turf
104	104	*Callophyllis* sp.	no	producer	turf

105	104	*Chaetomorpha linum*	no	producer	thin turf
106	104	*Monostroma grevillei*	no	producer	blade
107	104	*Neorhodomela aculeata*	no	producer	turf
108	104	*Odonthalia floccosa* f. *comosa*	no	producer	turf
109	104	*Plocamium pacificum*	no	producer	thin turf
110	104	*Pterocladiella caloglossoides*	no	producer	thin turf
111	104	*Styela* sp.	no	consumer	animal
112	113	*Ceramium "codicola"*	no	producer	thin turf
113	113	*Ectocarpus* sp.	no	producer	thin turf
114	113	*Mesophyllum vancouveriense*	no	producer	crust
115	113	*Pterygophora californica*	no	producer	canopy
116	113	*Symphyocladiella dendroidea*	no	producer	animal

***** Pyropia spp. includes specimens identified as*Neoporphyra perforata* , *Pyropia abbottiae* ,*Pyropia fallax* , *Neopyropia fucicola* , *Pyropia gardneri* , *Pyropia pulchra* , and *Wildemania norrisii*

**** Barnacles include *Balanus glandula* + *Chthamalusdalli* + *Semibalanus cariosus*

Model structure and fit:

We ran HMSC models using the following setup: thin = 100, transient = 12,500, samples = 250. Using four chains to traverse parameter space and sample the posterior distribution of estimates, we obtained a total of 1,000 samples from each species, which we used in downstream analysis and interpretation. Gelman's diagnostic scores were largely within the range of acceptable values (98-99% of values were < 1.05), suggesting that we had reached convergence of the model. Examination of trace plots (not shown here) provided further support that chains were well mixed.

Fig. S7. Summary of temporal trends from HMSC analysis. Colors represent support for positive (red) or negative (blue) linear trends based on overlap of credible intervals with zero (grey). Predictions were averaged over eight uniformly spaced elevations between 61 cm and 382 cm above MLLWLT (69 cm, 113 cm, 158 cm, 202 cm, 246 cm, 290 cm, 335 cm, 379 cm), weighted by the proportion of sampled elevations in the dataset (proportion [?] 0.11, 0.17, 0.13, 0.24, 0.17, 0.09, 0.08).

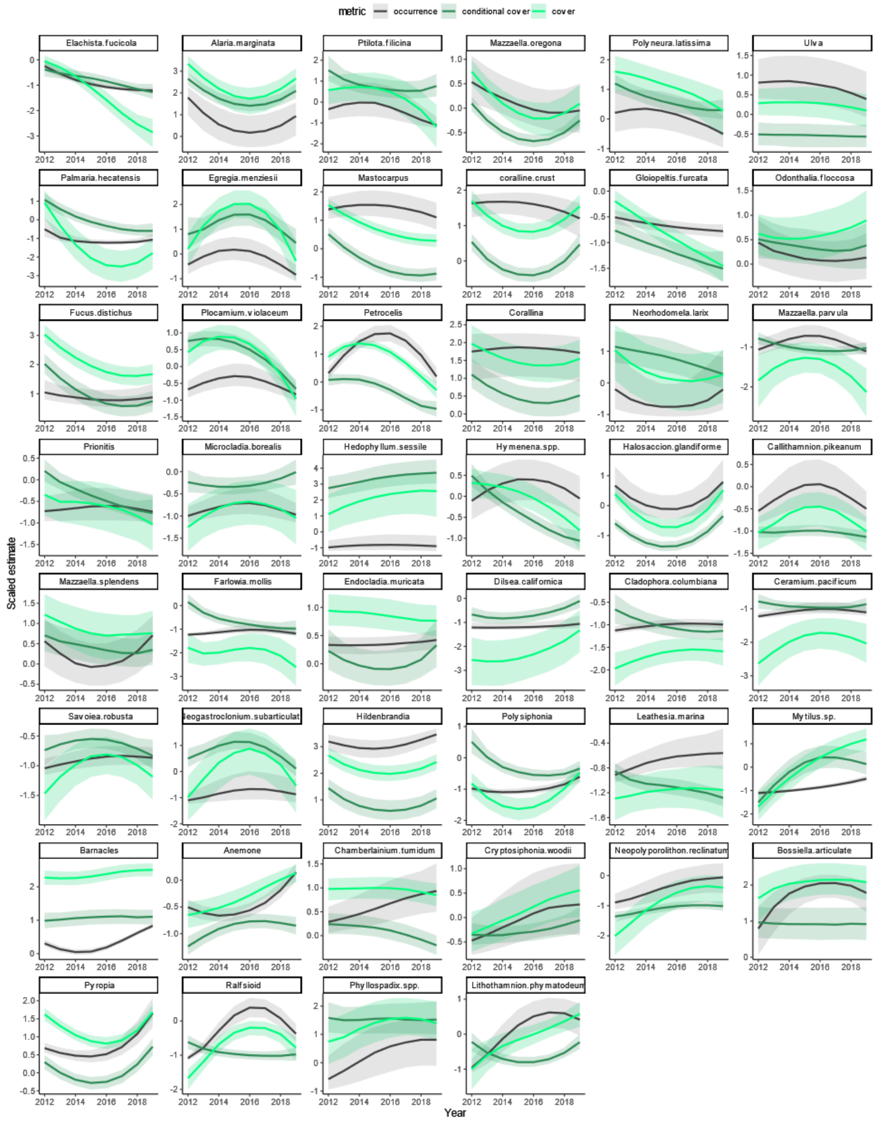

Fig. S8. Predictions from the HMSC hurdle model displaying scaled temporal trends for each taxon. Colors correspond to model metrics. Note that cover is produced by multiplying occurrence by conditional cover. Predictions were averaged over eight uniformly spaced elevations weighted by the frequency (see Fig. S7).

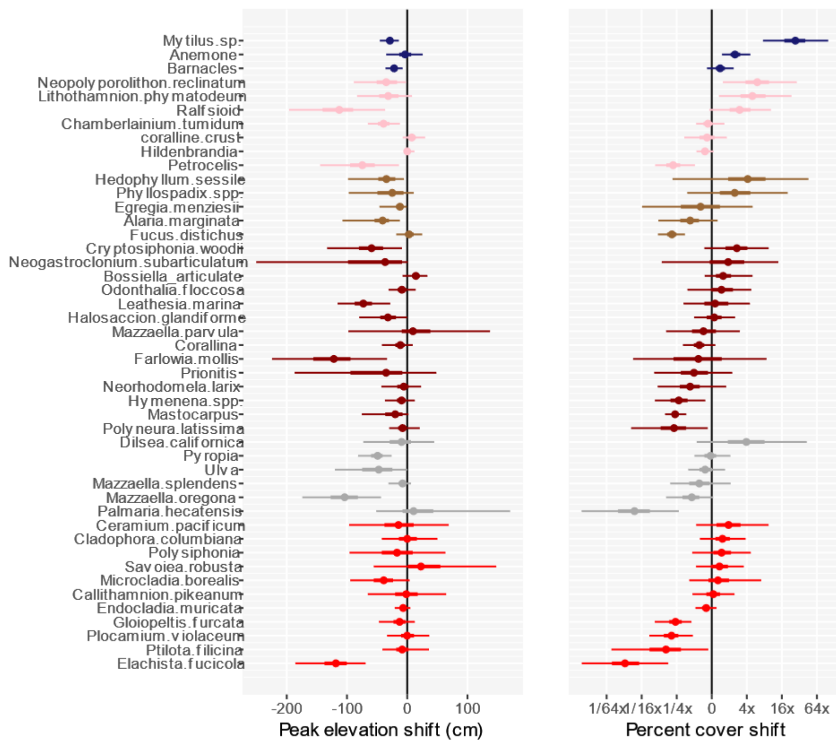

Fig. S9. Shifts in peak elevation (cm) and abundance (fold change) for the 46 taxa we modelled with HMSC, arranged by functional group and then individual trends in occurrence. Points are median shifts across 1,000 posterior samples (shown in Figure 2C), and errors bars are 50% (thick bars) and 95% CIs (thin bars). We constrained our predictions to the surveyed elevation range (61 to 382 cm above MLLWLT), creating a few situations where upper 95% credible limits for peak elevation shifts were exactly zero (e.g., *Egregia menziesii* , *Ulva* ,*Halosaccion glandiforme*). We do not consider these shifts to be significantly different from zero. Taxa are arranged from the greatest cover loss over time to greatest cover increases, first by functional group (colors as in Fig. 2) and then by taxa within functional groups.

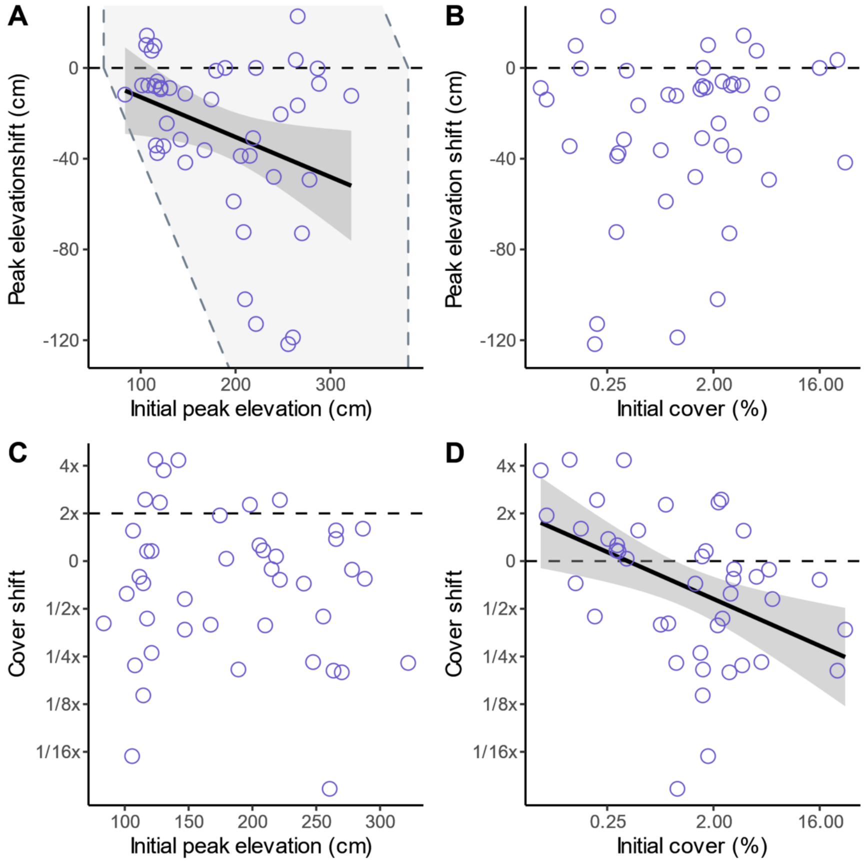

Fig. S10. Relationships among initial states and shifts over time for abundance and elevation as predicted by HMSC. Because our sampling design does not cover the entire elevation/depth distribution of every species, predicted elevational peaks for several species found below the lowest survey points (e.g., surfgrasses) or above the highest points (e.g., barnacles) were beyond the limits of the study area. We decided to restrict our predictions to the boundaries of the survey area. Therefore, the amount each taxon could shift up or down depended on its initial state (bounding box in A).

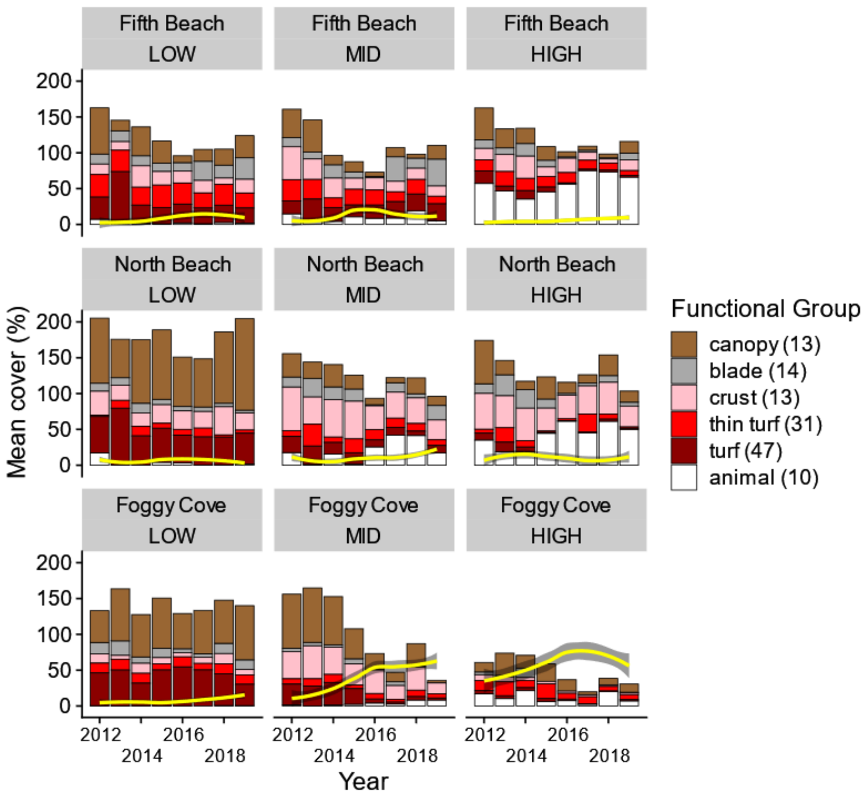

Fig. S11. Comparison of algal functional group dynamics and trends in bare rock cover. Mean abundance within functional groups (bar colors) is shown for each year of the time series. Numbers in parenthesis are counts of taxa in each group. Yellow lines show trends in bare rock cover based on local regressions (LOESS) with shaded 95% confidence intervals.

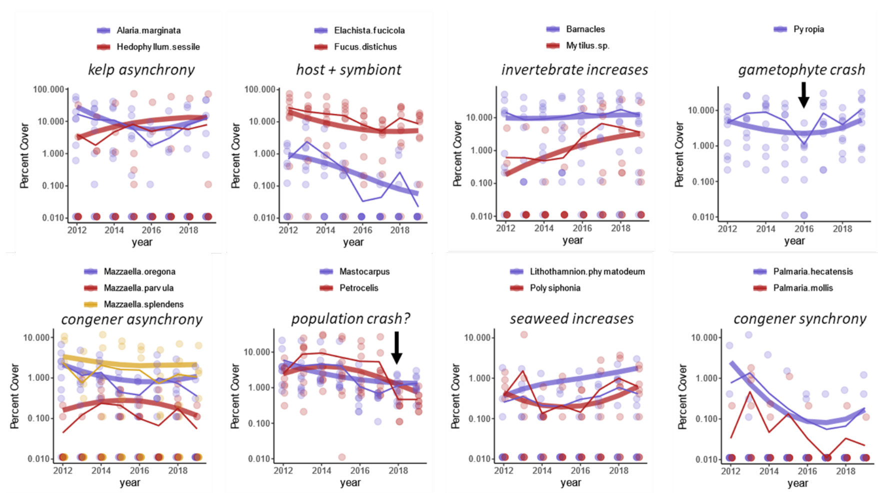

Fig. S12. Select time series of invertebrates and seaweeds observed during surveys. Thin lines show empirical annual means, while thick lines show mean cover predictions for taxa included in the HMSC analysis. HMSC predictions are averages over eight discrete elevations, weighted by their frequency of sampling in the dataset.

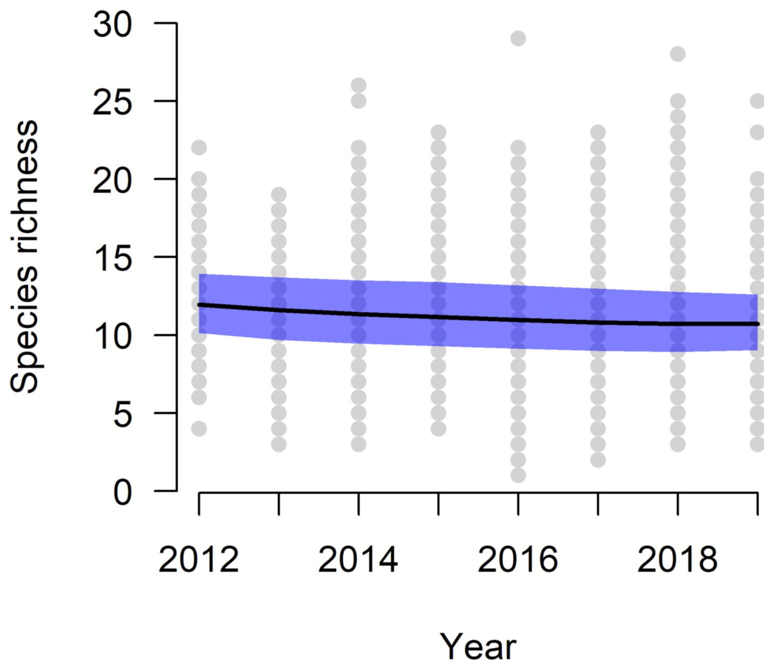

Fig. S13. Species richness estimate from the probit HMSC model (46 of 116 taxa).

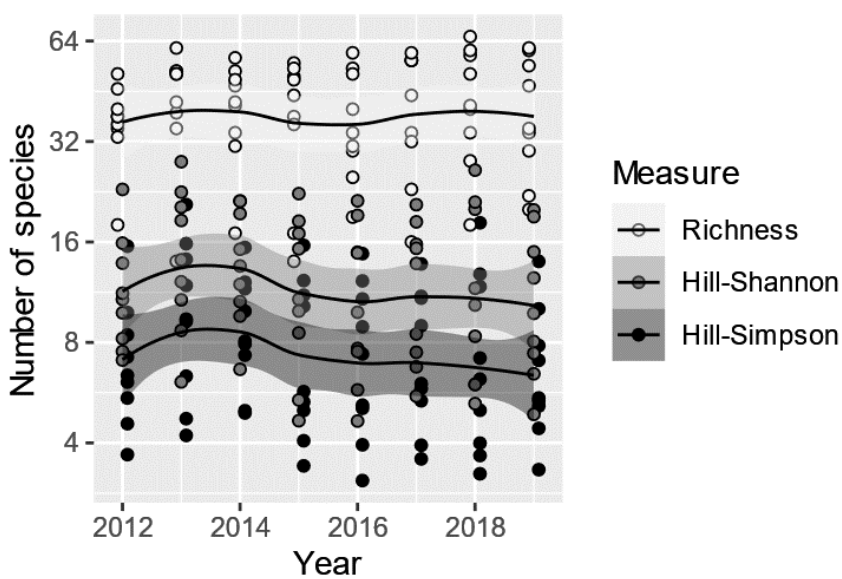

Fig. S14. Patterns of diversity expressed as three Hill numbers: species richness (white), Hill-Shannon index (light grey) and Hill-Simpson index (dark grey). Points are diversity values calculated from mean abundance of each taxon on each transect in each year, and lines show LOESS smooths with 95% confidence intervals independently fitted for each diversity measure. Note that y-axes are displayed on a $\log_2$ scale.

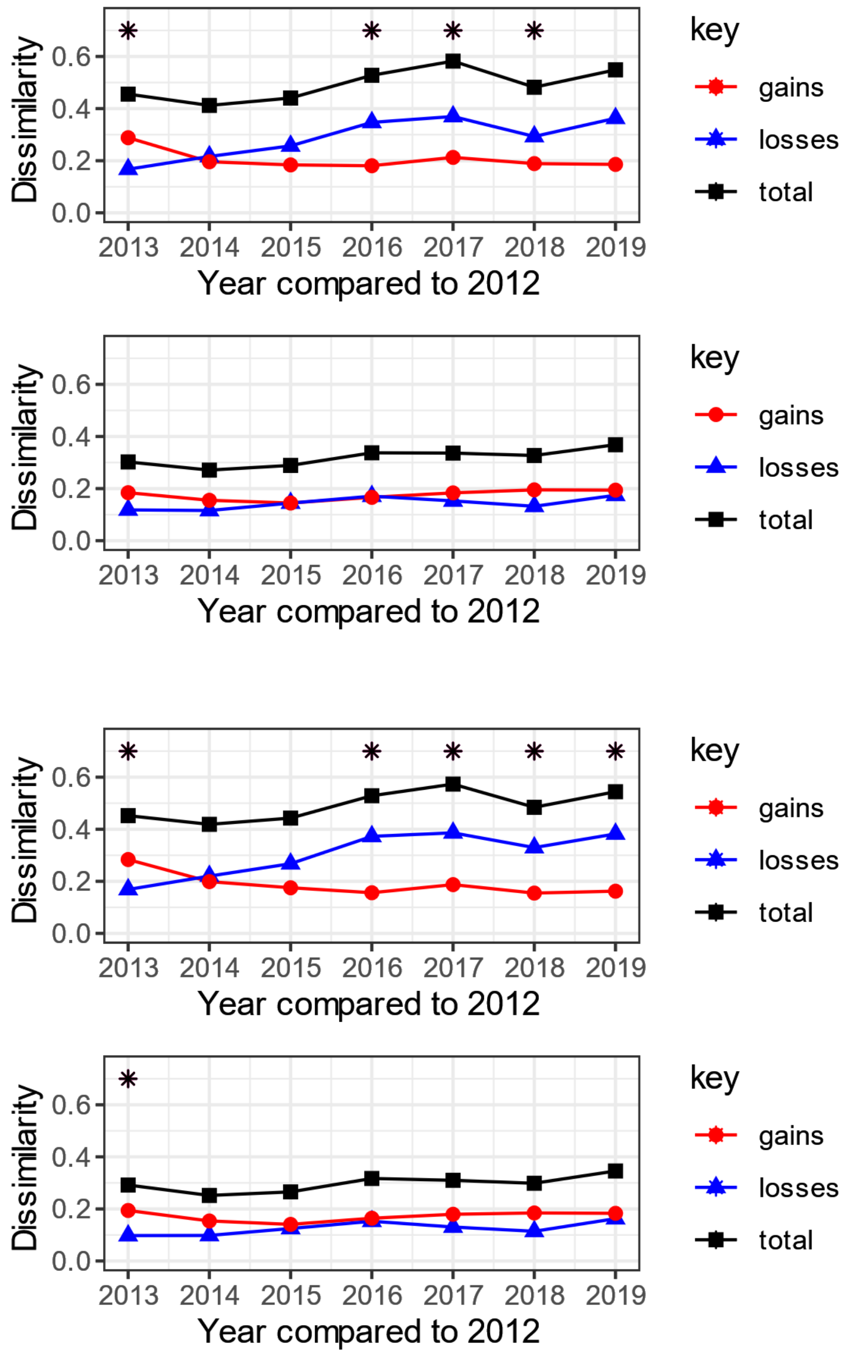

Fig. S15. Partitioning of temporal beta diversity indices within transects between years (left panels: all taxa; right: only seaweeds). The survey in 2012 is compared to each subsequent year in the dataset. Changes in dissimilarity were calculated using abundance data (top) and presence-absence data (bottom). Asterisks denote significant differences between gains and losses for each pair of years.